Journal of Polymers and the Environment (2020) 28:1766–1775
https://doi.org/10.1007/s10924-020-01725-8

ORIGINAL PAPER

Microcrystalline Cellulose from Fruit Bunch Stalk of Date Palm: Isolation and Characterization

Majed D. Alotabi[1] · Basheer A. Alshammari[2] · N. Saba[3] · Othman Y. Alothman[4] · Lau Kia Kian[3] · Anish Khan[5,6] · Mohammad Jawaid[3,4]

Published online: 5 April 2020

Abstract
Present study deals with the extraction and isolation of microcrystalline cellulose (MCC) from date palm fruit bunch stalk (DPFS) of date palm tree (*Phoenix dactylifera* L.) through integrated chemical method. To facilitate comparative study, each DPFS-treated, DPFS-pulp and DPFS-MCC samples were produced through respective bleaching, alkaline and acid hydrolysis treatments. The obtained samples were characterized in aspects of structural, morphological, elemental, crystallinity and thermal properties. From physicochemical analysis, fourier transform infrared ray (FTIR) and X-ray diffraction (XRD) showed the improved cellulose crystalline structure from DPFS-treated to DPFS-MCC. Morphology analysis revealed that the isolated DPFS-pulp and DPFS-MCC samples had microfibrillar structure, which achieved through the fibre disintegration by a series of chemical treatments. Moreover, the rigidity was also found the highest for isolated DPFS-MCC with 79.4% crystallinity degree. Further, the DPFS-MCC sample manifested better thermal properties for its high weight loss (84.15%), low residual weight (15.44%) and high decomposition temperature (364.2 °C) compared to the other fibre samples. Also, the DSC analysis showed the thermal behaviour which is in line with the thermal decomposition of those fibre samples. Therefore, in view of the overall result, the isolated DPFS-MCC could act as potential filler for reinforcing polymeric materials in composite field of applications.

Keywords Date palm tree · Fruit bunch stalk · Pulp bleaching · Acid hydrolysis · Microcrystalline cellulose

Introduction

Cellulose is a plant polymer that is both biodegradable as well as renewable and that has the potential to be processed into micro fibrils with whisker-like appearance [1, 2]. Among the remarkable traits that it possesses is the advantage of reinforcing capability, low density, environmental friendly nature and interesting mechanical properties [3]. These traits have caused scientists to be particularly interested in the plant polymer aiming to exploit it in developing green polymer composites that are environmentally friendly [4]. Cellulose is also regarded as the most ubiquitous and abundant natural polymers that produced by plants and microorganisms [5]. It is a linear homopolymer with formula of (C6H10O5)n in 4C1 conformational structure The repeating units which made up of d-glucose that does not dissolve in water but can be degraded by fungal and microbial enzymes [6, 7]. Naturally, the molecular chains of cellulose are biosynthesized and through self-assembly, they

✉ Mohammad Jawaid
jawaid_md@yahoo.co.in

1 Life Science and Environment Research Institute, King Abdulaziz City for Science & Technology, Riyadh, Saudi Arabia

2 National Center for Petrochemicals, Materials Science Institute, King Abdulaziz City for Science and Technology, Riyadh, Saudi Arabia

3 Department of Biocomposite Technology, Institute of Tropical Forestry and Forest Products, Universiti Putra Malaysia, UPM Serdang, Selangor, Malaysia

4 Department of Chemical Engineering, College of Engineering, King Saud University, Riyadh, Saudi Arabia

5 Center of Excellence for Advanced Materials Research, King Abdulaziz University, P.O. Box 80203, Jeddah 21589, Saudi Arabia

6 Chemistry Department, Faculty of Science, King Abdulaziz University, P.O. Box 80203, Jeddah 21589, Saudi Arabia

turn to microfibrils that are made up of crystalline as well as amorphous domains [8, 9].

Hydrogen bonds laterally stabilize the molecules of cellulose via hydroxyl groups that aligned between adjacent molecules [9]. Subjecting native cellulose of its amorphous regions to strong acid hydrolysis results in them being seamlessly hydrolyzed with close to no weight being lost [10]. Usually, the utilization of wood yields hydrolyzed cellulose could produce microfibrils with approximately 3–10 nm in width and 100–300 nm in length. The microparticles are given the term of 'microcrystalline cellulose' due to the possession microscale dimension [11–13]. Microcrystalline cellulose (MCC) refers to a crystalline powder as well as biodegradable material that is fine, has no order, is white and it can be removed from cellulose for use in water retention and as a suspension stabilizer in three major industries; pharmaceuticals, food and cosmetics [14, 15]. MCC for industrial use is collected by hydrolyzing wood as well as cotton cellulose primarily by use of dilute mineral acids [16]. High crystallinity degree is a typical characteristic of MCC although variations occur between MCC grades with values often ranging from 50 to 80 percent as is identified through X-ray diffraction examination [14]. When cellulose is collected from different hydrolysis conditions and origins, its crystallinity, particle size, surface area, molecular weight, porous structure and moisture content may vary accordingly [6, 13, 15].

Researchers have in the recent past reported that cellulose fibers can be extracted from rice husk through alkali as well as bleach treatments and using sulfuric acid (H_2SO_4) hydrolysis treatment, conversion of the cellulose fibers to nanocrystals was possible [17]. That same technique of acid hydrolysis has been found to isolate microcrystalline cellulose from jute cellulose [18]. Researcher has also used hydrolysis to produce cellulose nano fibres from empty fruit bunch fibers of oil palm [19]. Additionally, there have been reports of synthesis as well as characterization of cellulose phosphate that have been obtained from microcrystalline cellulose that is derived from oil palm empty fruit bunch [20, 21]. In the past few years, interest has grown significantly on production of nanocomposite materials. Such interest is linked with the extraordinary properties that the nanocomposite materials exhibit based on nanoscale reinforcement that provides properties like increased surface area which enhances bonding with resins and creates optical transparency in addition to other properties such as electrical conduction. For nanocomposites that are fully renewable as well as biodegradable to be produced, derivation of both nano reinforcement and polymer matrix needs to be done from resources that are renewable [22, 23]. Researchers are increasingly becoming interested in MCC particularly on its potential use with cellulose reinforced nanocomposite as a starting material [24]. Additional reports indicate that the characteristics of MCC are depending on the origin of raw materials as well as the employed methods in their preparation steps [25].

All the findings indicate the possible use of MCC as universal filler during the process of extrusion or spheronisation. Unique mechanical properties of cellulose nanofibers have been displayed including their high modulus of approximately 140 GPa [26]. Further, they represent ideal materials to utilize as reinforcement in the context of a transparent polymeric matrix largely due to their capacity to avoid light scattering. Inability to scatter light is associated with their lateral dimensions which are smaller compared to visible light's wavelength [27]. Characterization of isolated MCC from OPEFB in a comprehensive manner or comparing it with commercial MCC as well as OPEFB-pulp has been achieved by using oil palm biomass residue as the raw cellulosic material [28]. Some of the recently reported studies on the isolation of MCC from natural fiber and wastes are listed in Table 1.

Table 1 Reported study on MCC isolation from natural source

MCC-source	Isolation methods	References
Indonesian native oil palm empty fruit bunch	Acid hydrolysis	[29]
Roselle fiber	Acid hydrolysis	[30]
Oil palm empty fruit bunches, stalk and spikelet	Acid hydrolysis	[31]
Pre-hydrolysed oil palm fronds wastes	Chemo-mechanical process	[32]
Recycled waste of cotton fabrics	Catalytic hydrolysis of phosphotungstic acid	[33]
Oil palm fronds waste	Acid hydrolysis	[34]
Pomelo peel	Acid hydrolysis	[35]
Alfa fibres or esparto grass	Acid hydrolysis	[36]
Waste papers	Acid hydrolysis	[37]
Banana fibre wastes	Acid hydrolysis	[38]
Ensete glaucum (Roxb.)	Acid hydrolysis	[39]
Rice husk	Chlorine-free multiple steps	[40]

From the literature review, it is known that the isolation and characterization of MCC from wood, cotton, jute, coir, flax and roselle has been reported. However, no studies have been focused on date palm fruit bunch stalk as a source of cellulose more specifically MCC. Most probably the present study for date palm and its findings will fill a knowledge gap for MCC extraction from other cellulose sources. With this regard, this work was performed to isolate and characterize MCC from fruit bunch stalk (DPFS) obtained from date palm tree through acid hydrolysis followed by its comparative study with DPFS-treated and DPFS-pulp. DPFS-MCC was fully characterized in terms of structural, morphological, elemental, crystallinity and thermal stability. Hence, the novelty of this work emphasizes on the utilization of DPFS as a new raw material for isolating MCC product.

Materials

DPFS were supplied from Riyadh, Saudi Arabia. Through water retting technique, extraction of the fruit bunch stalks fiber was done. In order to remove impurities, fiber were thoroughly washed with tap water and dried in an oven for 24 h at 60°, followed by grounding and sieving to around 10 mm size of dried of fruit bunch stalk fiber. Sodium hypochlorite, hydrochloric acid, acetic acid and sodium hydroxide were procured from Evergreen Sdn. Bhd. Malaysia.

Methods

Preparation of MCC

Firstly, extraction of MCC involved the bleaching treatment of fiber by using 10.0 (w/v) sodium hypochlorite (NaClO) solution for an hour and at temperatures ranging between 70–80 °C. The ratio of fiber to NaClO was 1:60 (g/ml) and acidification of the solution was done using acetic acid until a pH of 4 was achieved. Bleached fibers were filtered after washing several times with distilled water until white-yellowish fibers are collected followed by drying it in oven for 24 h at 60 °C. Bleached fibers were then treated with 8.0% (w/v) of sodium hydroxide (NaOH) solution based on a 1:50 (g/ml) fiber to NaOH ratio for 30 min at room temperature. Alkali treated bleached pulp was filtrated, washed and then dried in an oven for 24 h and at 60 °C.

The next step involves hydrolyzing of the alkali treated bleached pulp by using 2.5 mol/L of hydrochloric acid for 30 min, at 85 °C based on a 1:30 (g/ml) solid to liquor ratio [14, 41], with constant stirring for hydrolysis agitation, followed by cooling at ambient temperature. Cooled hydrolyzed alkali treated bleached pulp were washed with distilled water, filtered and washed until a pH of 7 was achieved, to obtain MCC. Isolated MCC was then put in a vacuum oven where it dried at temperatures between 70–80 °C for 5 h until constant weight was reached.

Characterizations

Chemical Composition and Yield Determination

Chemical composition of fiber samples (α-cellulose, hemicellulose and holocellulose) were determined accordingly to the TAPPI test methods: holocellulose by Tappi 249-75, α-cellulose by T203cm-99, and lignin by TAPPI T222 om-88. Meanwhile, hemicellulose was calculated by subtracting the content of holocellulose with α-cellulose.

The fiber yield (%) was estimated following the Eq. (1) provided:

$$Yield(\%) = \frac{(M_2 - M_3)}{M_1} \times 100\% \quad (1)$$

where M_1 refers the mass of raw date palm fruit bunch stalk; M_2 refers the total mass of chemically-treated fiber in weighing bottle; M_3 refers the mass of weighing bottle.

FT-IR

FT-IR was done by conducting 32 scans through Perkin Elmer 1600 Infrared spectrometer ranging of 450–4000 cm^{-1} wavenumbers at a resolution of 4 cm^{-1} for the individual samples. Nicolet software was used to track the significant transmittance peak position recorded for a specific wave number.

SEM, EDX and Particle Size Analysis

A Hitachi S-3400 N SEM was used to observe the morphology of the samples equipped with EDX under 15 kV of accelerating voltage. Prior to scanning sample were coated with gold sputter in order to avoid charging effect. EDX diffraction determines the sample elemental composition. Particle size analysis was done through an effective particle size analyzer called the Malvern Mastersizer 2000.

XRD

A SIEMENS D5000 XRD was used to identify the samples crystallinity by employing Ni-filtered Cu Ka radiation under angular incidence (2θ angle range 5°–40°). The diffraction peak height intensity method Eq. (2) was used to calculate the samples' Crl (crystallinity index).

$$\mathrm{CrI}(\%) = \frac{I_{002} - I_{am}}{I_{002}} \quad (2)$$

where, I_{002} refers to the peak intensity that corresponds to crystalline domain at about 2θ = 19.0°, while I_{am} refers to the peak intensity that corresponds to amorphous domain at about 2θ = 22.6°.

Thermal Analysis

Thermal stability of the samples was done through TA Instruments Q500. Approximately 6 mg of the sample was put under a nitrogen gas atmosphere with heating rate of 20 °C/min and scanned in the range of 30–900 °C. Differential scanning calorimeter (DSC) thermograms of 10 mg of dry sample were recorded through TA Instruments Q20 based at heating rate of 10 °C/min under nitrogen purge with temperature range of 30–350 °C.

Results and Discussion

Physicochemical, Chemical Composition, and Yield Production

Figure 1 illustrates the FTIR spectra of three samples DPFS-treated, DPFS-pulp and DPFS-MCC. At different absorbance bands, the samples manifest differences in reactions to chemical treatments. For instance, at approximately 3290 cm^{-1}, it represents –OH stretching group on cellulose chain. The degree of changes for the individual samples throughout the chemical treatments is insignificant, while similar outcome is identified at 2896 cm^{-1} absorbance band. From the Fig. 1, it is also observed the absorbance band peak around 1640 cm^{-1} broadens from DPFS-treated to DPFS-MCC largely due to increased cellulose-water interactions strength. Moreover, pure cellulose and its common characteristics are represented at three key absorbance peaks, namely; 898 cm^{-1}, 1157 cm^{-1} and 1365 cm^{-1} which can also be referred to as 'β-glycosidic linkage vibration', 'C–O–C pyranose ring skeletal vibration' and 'C–H asymmetric vibration' respectively [28].

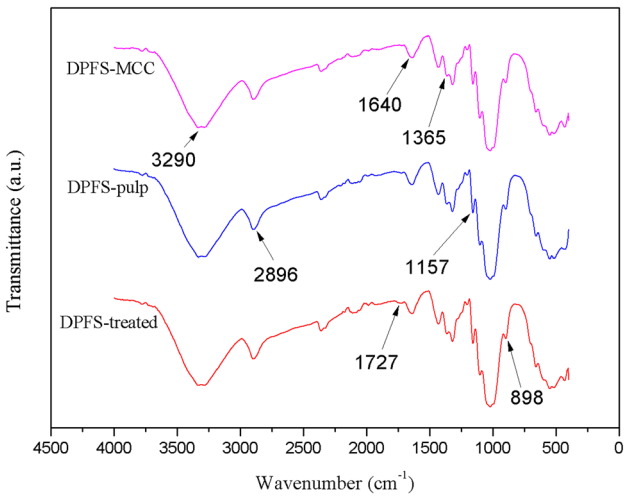

Fig. 1 FTIR spectra of DPFS-treated, DPFS-pulp and DPFS-MCC

With regards to the DPFS-treated sample, a small peak is seen at 1727 cm^{-1} which might be considered as an indication that hemicellulose is present following the alkaline reaction. However, for DPFS-pulp and DPFS-MCC, that peak is less likely to be seen because substantial hemicelluloses has been removed after the bleaching as well as hydrolysis treatments have been done. Interestingly, almost complete elimination of lignin compound that occur during alkaline treatment make it insignificant to observe any of the related peaks from 1510 to 1610 cm^{-1} in all the samples (C=C aromatic stretching) [42, 43]. This observation was strongly supported by the determined chemical composition as summarized in Table 2. The α-cellulose was found increasing from DPFS-treated to DPFS-MCC samples with the declined hemicellulose and lignin components. Also, the yield of MCC could be extracted in this work was with a total of 35.4%.

Morphology, Element and Particle Size Analysis

Figure 2 illustrates SEM images of the DPFS-treated, DPFS-pulp and DPFS-MCC. Initially, the DPFS-treated sample shows its fibre in a bundle-like feature and reflects a relatively smooth surface following an alkaline treatment reaction. With further bleaching treatment, the residual component of DPFS-treated fibre was dissolved and hence resulting in the fibre disintegration into individualized form of DPFS-pulp. As for the isolated DPFS-MCC sample, similarity with the DPFS-pulp sample is manifested with regards to the long microfibrillar structure that it achieves through self-assembly. A difference is however manifested between the DPFS-MCC and DPFS-pulp samples as the former has a rougher surface than the latter partly because of acid hydrolysis and the surface cracking caused by the disruption [44, 45]. Moreover, the dimension of MCC extracted in this

Table 2 Chemical composition and yield data

Samples	α-Cellulose (%)	Hemicellulose (%)	Lignin (%)	Yield (%)
DPFS-treated	71.2	14.2	9.4	57.1
DPFS-pulp	74.7	13.6	7.9	52.2
DPFS-MCC	82.5	5.11	3.6	35.4

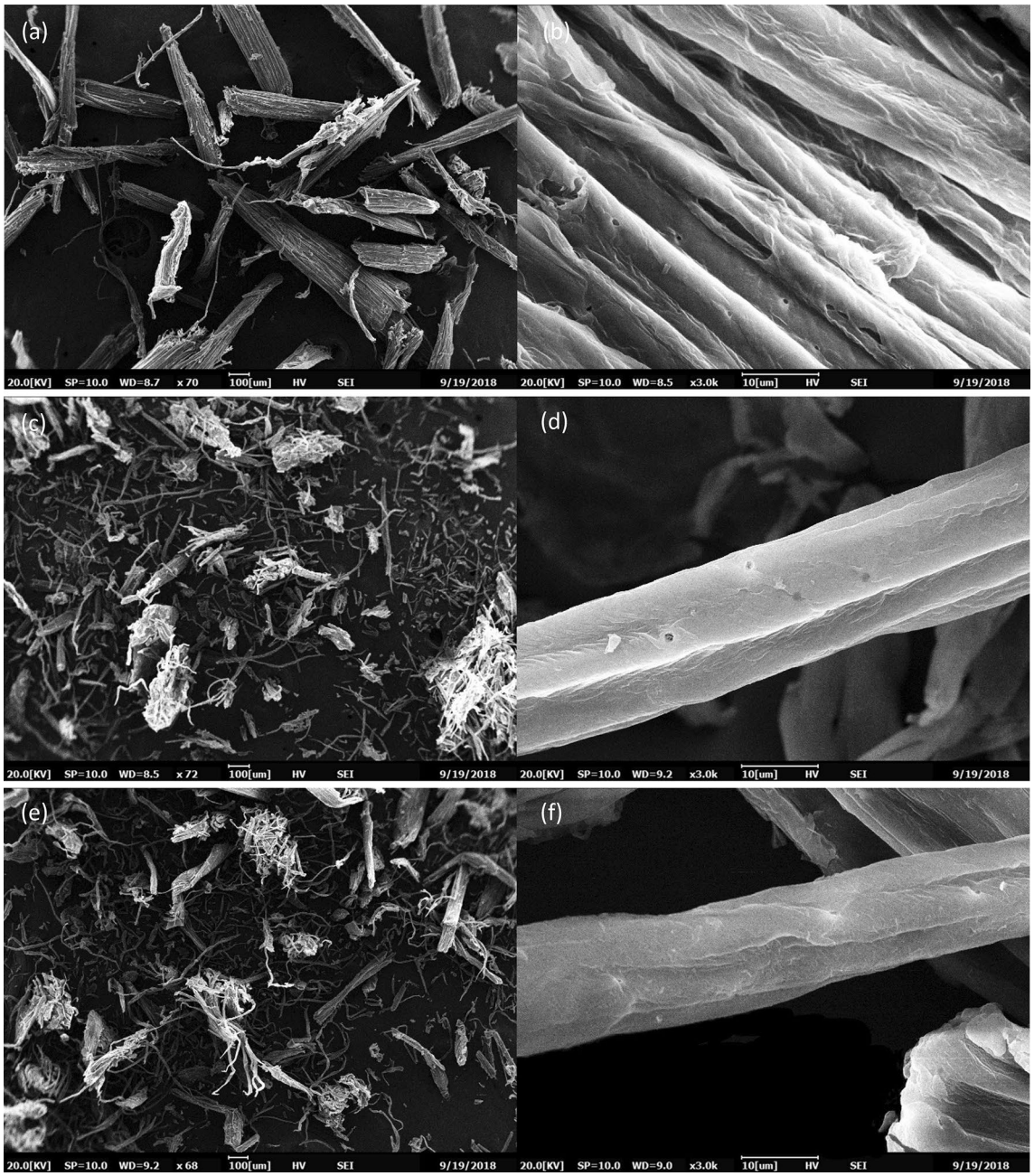

Fig. 2 SEM of DPFS-treated (**a**, **b**), DPFS-pulp (**c**, **d**) and DPFS-MCC (**e**, **f**) at magnifications of ×70 (**a**, **c**, **e**) and ×3000 (**b**, **d**, **f**)

work had diameter of 21.4–90.6 µm and length of more than 200 µm. The size of MCC obtained in this work was larger than the reported works of alfa MCC (5 to 10 µm diameter, 20 to 200 µm length) extracted by Trache et al. [16], soybean hull MCC (13 ± 3 µm diameter, 48 ± 16 µm length) by Merci et al. [44], and rice straw MCC (15–20 µm diameter, 100–1000 length) by Elanthikkal et al. [38]. However, the large dimension range of DPFS-MCC could more likely to improve the composite strength during reinforcement.

Figure 3 shows EDX spectra of three samples DPFS-pulp, DPFS-treated and DPFS-MCC. Figure 3 clearly indicate that every fiber from the three samples shows peaks for oxygen as well as carbon elements as being the key composition correlating to the natural characteristics of cellulose as listed in Table 3. In addition, phosphorus as well as silica impurity elements were present in negligible amounts in the fibre samples. As such, through EDX analysis, it was shown that the cellulose content in the individual fiber has high purity

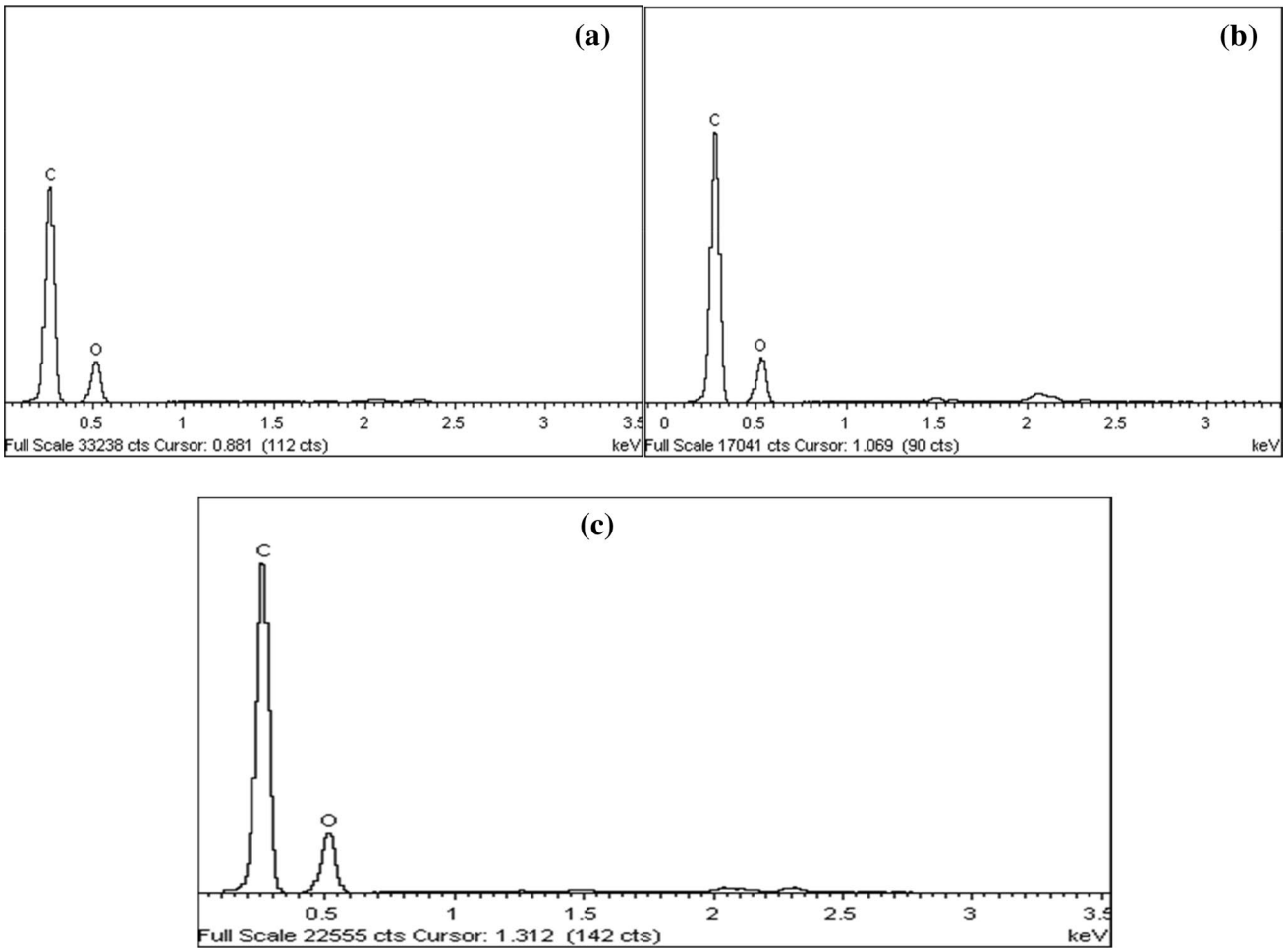

Fig. 3 EDX spectra of **a** DPFS-treated, **b** DPFS-pulp and **c** DPFS-MCC

Table 3 Elemental, particle size and crystallinity data of DPFS-treated, DPFS-pulp and DPFS-MCC

Samples	C (%)[a]	O (%)[b]	SWMD (μm)[c]	VWMD (μm)[d]	CrI (%)[e]
DPFS-treated	63.48	36.52	270.19	411.13	74.6
DPFS-pulp	65.65	34.35	73.24	287.25	76.5
DPFS-MCC	65.16	34.84	71.92	259.32	79.4

[a]Carbon

[b]Oxygen

[c]Surface weighted mean diameter

[d]Volume weighted mean diameter

[e]Crystallinity index

after alkaline, bleaching and acid hydrolysis treatments have been performed in respective fashion [46, 47].

Figure 4 elucidates the distribution of particle size in all the three samples under investigation. The pattern shows

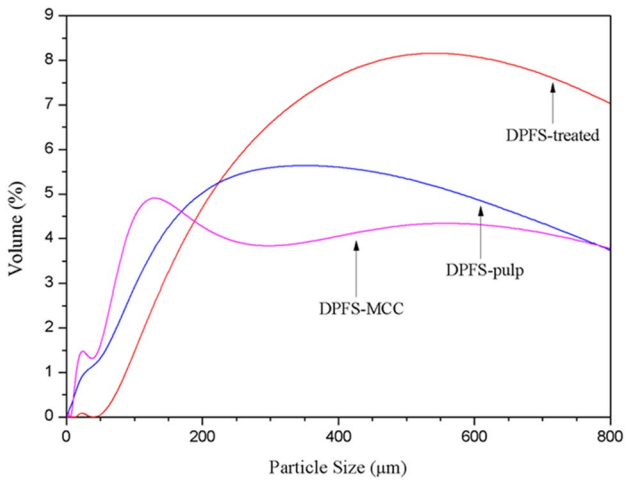

Fig. 4 Particle size distribution of DPFS-treated, DPFS-pulp and DPFS-MCC

that there is a decline in volume weighted mean diameters as one moves from DPFS-treated to DPFS-pulp samples. Manifested pattern observed as large cellulosic bundles gets separated into fibrous strands that are smaller after the hemicelluloses and lignin binding components have been removed in the alkaline treatment.

The volume weighted mean diameter of DPFS-MCC with 259.32 µm declines slightly following acid hydrolysis treatment to DPFS-pulp with 287.25 µm. The pattern exhibited by DPFS-MCC was corresponding to the mild decline in surface weighted mean diameters from 73.24 µm for the DPFS-pulp sample to 71.92 µm for the DPFS-MCC sample (Table 3). The inference agreed with the fact that the hydrolytically cleavage of cellulose amorphous segments had contributed to the formation of smaller DPFS-MCC microcrystallites. Moreover, the size distribution of DPFS-MCC samples is unsymmetrical relative to that of DPFS-pulp as shown in Fig. 4 because of inconsistent size reduction resulted by the acid attack on the glyosidic bonds [32].

XRD

XRD patterns of DPFS-treated, DPFS-pulp and DPFS-MCC are shown in Fig. 5. Each of the samples shows their main peaks of reflections in correspondence with their respective crystallographic planes. Table 3 listed the crystallinity degree (%) of DPFS-treated, DPFS-pulp and DPFS-MCC. Meanwhile, the main peaks reflected that the individual samples have cellulose Iβ type structure [34]. Crystallinity degree was presented higher for DPFS-pulp with 76.5% when in comparison with DPFS-treated having crystallinity of 74.6%. Noticeably, the peak became sharper and narrower at 22.8° from DPFS-treated to DPFS-pulp fibres. The variation in peaks and crystallinity occurred between them because the amorphous cellulose content was eliminated in DPFS-treated fibre causing crystallinity to increase. In addition, the highest crystallinity is 79.4% which exhibited by DPFS-MCC. The contributing factor is the fragmentation of amorphous segments in cellulose by hydronium ions attack occurred during acid hydrolysis and thereby resulted in crystalline structure in highly ordered [31, 47]. The MCC isolated from date palm empty fruit bunch fibre in this study had a greater crystallinity degree than the jute MCC produced by Jahan et al. [18] with 75% crystallinity index. Also, this work had greater MCC crystallinity comparing to Merci et al. [44] by which the isolation of 70% crystallinity of soybean hulls MCC using reactive extrusion.

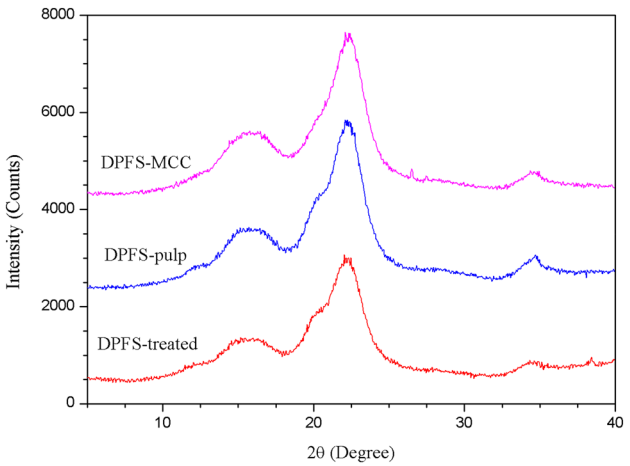

Fig. 5 XRD plots of DPFS-treated, DPFS-pulp, and DPFS-MCC

Thermal Properties

Figure 6a illustrates TGA curves for DPFS-treated, DPFS-pulp and DPFS-MCC. Loss of weight from 70 to 130 °C is observed due to the evaporation of absorbed water for each sample. Beyond 200 °C, the thermal decomposition begins at 272.6 °C for DPFS-treated fibre which represents a lower thermal stability compared to DPFS-pulp at 235.3 °C and DPFS-MCC at 251.8 °C, respectively (Table 4). It is probably caused by the residual hemicelluloses and lignin content in DPFS-treated fibre that had increased the tolerance to heat degradation. Apart from this, it might be also attributed by its bundle-like structure which improved its thermal stability [48]. The initial thermal decomposition found poor in DPFS-pulp compared to DPFS-MCC most probably because the cellulose amorphous regions easily get degraded in DPFS-pulp. However, the weight loss was lowest in DPFS-treated at 83.91% but residual weight was highest at 16.03% compared to the other samples probably because of the formation of char due to the presence of undecomposed components [49]. Additionally, weight loss was observed to be highest in the DPFS-MCC at 84.15% most likely because the relatively high content of pure cellulose. Residual weight in DPFS-MCC was also found to be slightly higher than in DPFS-pulp probably because the crystalline structure of DPFS-MCC exhibits flame retardant behaviour [16]. From derivative thermograms (DTG) as illustrated in Fig. 6b, double thermal decomposition was only observed for DPFS-treated fibre at 265.4 °C and 359.9 °C probably due to the fibre contained unremoved impurity such as hemicelluloses. The peak temperature of decomposition was higher in the DPFS-MCC at 364.2 °C compared to 350.4 °C for DPFS-pulp. This shows that the heat resistance capability is remarkable in the DPFS-MCC due to the presence of rigid crystals [50].

Figure 7 illustrates the DSC plots and the data are tabulated in Table 4. Absorption of heat energy in the individual samples for the process of water evaporation was noticed to occur from 60 °C to 140 °C endotherms. Second endotherms were observed at 206.6 °C for DPFS-treated, 204.3 °C, 205.8 °C for DPFS-pulp and DPFS-MCC respectively which

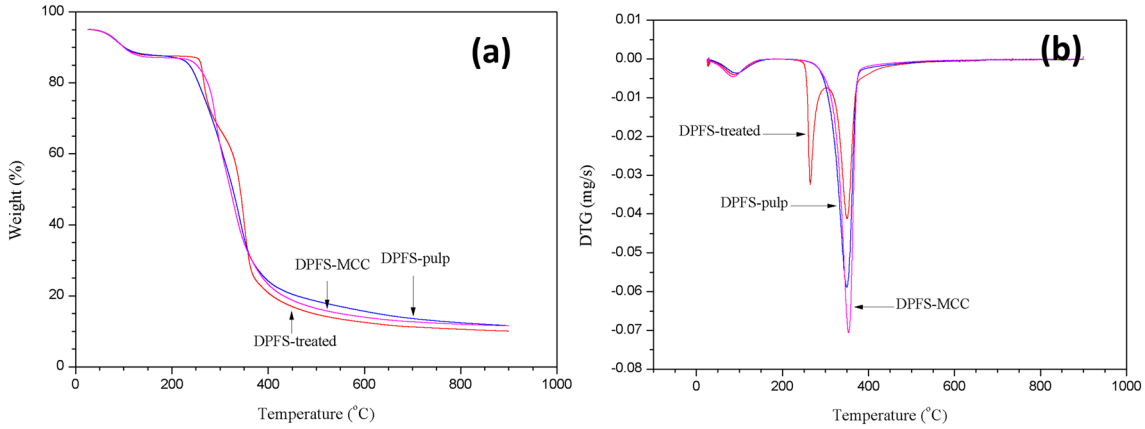

Fig. 6 **a** TGA curves and **b** DTG curves of DPFS-treated, DPFS-pulp and DPFS-MCC

Table 4 Thermal analysis data of DPFS-treated, DPFS-pulp and DPFS-MCC

Samples	TGA analysis				DSC analysis		
	T_{onset} (°C)[a]	T_{peak} (°C)[b]	W_{loss} (%)[c]	$W_{residue}$ (%)[d]	T_{onset} (°C)[e]	T_{peak} (°C)[f]	ΔH (J/g)[g]
DPFS-treated	272.6	359.9	83.91	16.03	206.6	320.6	244.6
DPFS-pulp	235.3	350.4	84.04	15.44	204.3	319.5	138.5
DPFS-MCC	251.8	364.2	84.15	15.71	205.8	328.1	87.9

ΔH Enthalpy change

[a]TGA onset decomposition temperature

[b]DTG maximum weight loss peak temperature

[c]TGA weight loss

[d]TGA char residual weight

[e]DSC onset degradation temperature

[f]DSC peak temperature

[g]DSC heat of degradation

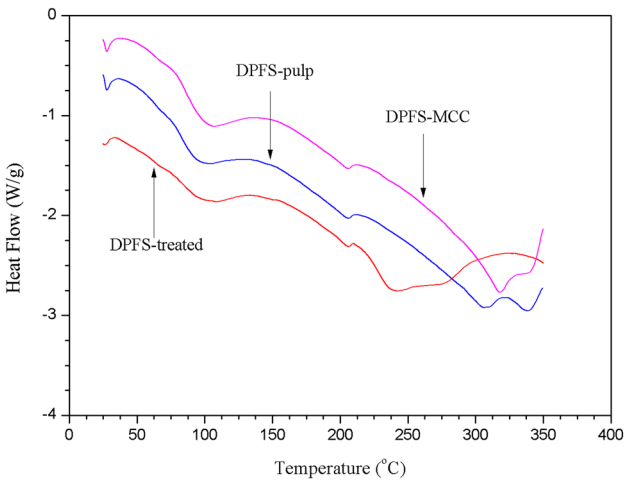

Fig. 7 DSC curves of DPFS-treated, DPFS-pulp and DPFS-MCC

is an indication that cellulose degradation has begun to prevail [34, 51]. When temperatures increased beyond 220 °C, the DPFS-treated sample showed a series of broad exothermic and endothermic peaks compared to the other two samples. As such, the amount of ΔH that is required for the DPFS-treated was quite high with approximately 244.6 J/g to undergo thermal degradation which is likely caused by the strongly interacted bundle structure. Further, cellulose decarboxylation and depolymerisation in DPFS-MCC consumed less ΔH of about 87.9 J/g compared to the ΔH for DPFS-pulp with about 138.5 J/g. This difference precisely associated with the binding capability between its contained particles and the amorphous domains which is more obvious in the DPFS-pulp fibre. The binding capability facilitated the formation of a structure that is strongly self-entangled. Moreover, the observed peak temperature is in relation to

maximum degradation proving that the DSC result was in agreement with TGA result [21, 52].

Conclusion

In this work successful attempt were made to isolate MCC through the integrated processes of bleaching, alkaline and acid disintegration from the fruit bunch stalk of date palm tree. That finding has strong implications on date palm trees which found abundance in Saudi Arabia. FT-IR analysis confirmed that the individual samples reacted differently to the performed chemical treatments, while the degree of changes associated with reaction to chemical treatments was irrelevant and insignificant. SEM analysis illustrate that the morphological structure of isolated DPFS-MCC with short micro-crystallites shape varies from long microfibrillar DPFS-pulp owing to hydrolytic fragmentation process. Moreover, crystallinity was the highest for DPFS-MCC with 79.4%, endowing it with rigidity for reinforcing composite during fabrication process. Thermal properties evaluation also proved that DPFS-MCC has relatively good thermal stability, suggesting it could withstand high temperature for various application purposes. The results generated prompt the researchers to conclude that production of DPFS-MCC through acid hydrolysis is quite facile and practical. Therefore, the extracted DPFS-MCC can be utilized as bio-reinforcing material for future nanocomposite fabrication process.

Acknowledgements The Authors would like to thank King Abdulaziz city for Science and Technology (KACST), and Universiti Putra Malaysia (UPM) for research support. The authors also extend their appreciation to the International Scientific Partnership Program ISPP at King Saud University for funding this research work through ISPP-0011.

References

1. Abraham E, Deepa B, Pothan L, Jacob M, Thomas S, Cvelbar U, Anandjiwala R (2011) Carbohydr Polym 86:1468–1475
2. Eichhorn SJ (2011) Soft Matter 7:303–315
3. Saba N, Safwan A, Sanyang M, Mohammad F, Pervaiz M, Jawaid M, Alothman O, Sain M (2017) Int J Biol Macromol 102:822–828
4. Einchhorn S, Dufresne A, Aranguren M, Capadona J, Rowan S, Weder C, Thielemans W, Roman M, Renneckar S, Gindl W (2010) J Mater Sci 45:1–33
5. Klemm D, Heublein B, Fink HP, Bohn A (2005) Angew Chem Int Ed 44:3358–3393
6. Li R, Fei J, Cai Y, Li Y, Feng J, Yao J (2009) Carbohydr Polym 76:94–99
7. Saba N, Mohammad F, Pervaiz M, Jawaid M, Alothman O, Sain M (2017) Int J Biol Macromol 97:190–200
8. Fernandes AN, Thomas LH, Altaner CM, Callow P, Forsyth VT, Apperley DC, Kennedy CJ, Jarvis MC (2011) Proc Natl Acad Sci USA 108:E1195–E1203
9. Nishiyama Y (2009) J Wood Sci 55:241–249
10. Rånby BG (1951) Discussions Faraday Soc 11:158–164
11. Goetz L, Mathew A, Oksman K, Gatenholm P, Ragauskas AJ (2009) Carbohydr Polym 75:85–89
12. Bras J, Hassan ML, Bruzesse C, Hassan EA, El-Wakil NA, Dufresne A (2010) Ind Crops Prod 32:627–633
13. De Menezes AJ, Siqueira G, Curvelo AA, Dufresne A (2009) Polymer 50:4552–4563
14. Chuayjuljit S, Su-uthai S, Charuchinda S (2010) Waste Manag Res 28:109–117
15. El-Sakhawy M, Hassan ML (2007) Carbohydr Polym 67:1–10
16. Trache D, Hussin MH, Chuin CTH, Sabar S, Fazita MN, Taiwo OF, Hassan T, Haafiz MM (2016) Int J Biol Macromol 93:789–804
17. Johar N, Ahmad I, Dufresne A (2012) Ind Crops Prod 37:93–99
18. Jahan MS, Saeed A, He Z, Ni Y (2011) Cellulose 18:451–459
19. Fahma F, Iwamoto S, Hori N, Iwata T, Takemura A (2010) Cellulose 17:977–985
20. Daud WRW, Kassim MHM, Mohamded MAS (2011) BioResources 6:1719–1740
21. Wanrosli W, Rohaizu R, Ghazali A (2011) Carbohydr Polym 84:262–267
22. Samir MASA, Alloin F, Dufresne A (2005) Biomacromol 6:612–626
23. Petersson L, Kvien I, Oksman K (2007) Compos Sci Tech 67:2535–2544
24. Mathew AP, Oksman K, Sain M (2006) J Appl Polym Sci 101:300–310
25. Lee SY, Mohan DJ, Kang IA, Doh GH, Lee S, Han SO (2009) Fibers Polym 10:77–82
26. Sturcová A, Davies GR, Eichhorn SJ (2005) Biomacromol 6:1055–1061
27. Yano H, Sugiyama J, Nakagaito AN, Nogi M, Matsuura T, Hikita M, Handa K (2005) Adv Mater 17:153–155
28. Haafiz MM, Eichhorn S, Hassan A, Jawaid M (2013) Carbohydr Polym 93:628–634
29. Pujiasih S, Masykur A, Kusumaningsih T, Saputra OA (2018) Carbohydr Polym 184:74–81
30. Kian LK, Jawaid M, Ariffin H, Alothman OY (2017) Int J Biol Macromol 103:931–940
31. Xiang LY, Mohammed MAP, Baharuddin AS (2016) Carbohydr Polym 148:11–20
32. Owolabi AF, Haafiz MM, Hossain MS, Hussin MH, Fazita MN (2017) Int J Biol Macromol 95:1228–1234
33. Hou W, Ling C, Shi S, Yan Z (2019) Int J Biol Macromol 123:363–368
34. Hussin MH, Pohan NA, Garba ZN, Kassim MJ, Rahim AA, Brosse N, Yemloul M, Fazita MN, Haafiz MM (2016) Int J Biol Macromol 92:11–19
35. Liu Y, Liu A, Ibrahim SA, Yang H, Huang W (2018) Int J Biol Macromol 111:717–721
36. Trache D, Donnot A, Khimeche K, Benelmir R, Brosse N (2014) Carbohydr Polym 104:223–230
37. Okwonna OO (2013) Carbohydr Polym 98:721–725
38. Elanthikkal S, Gopalakrishnapanicker U, Varghese S, Guthrie JT (2010) Carbohydr Polym 80:852–859
39. Pachuau L, Dutta RS, Hauzel L, Devi TB, Deka D (2019) Carbohydr Polym 206:336–343
40. Rosa SM, Rehman N, Miranda MIG, Nachtigall SM, Bica CI (2012) Carbohydr Polym 87:1131–1138
41. Chauhan Y, Sapkal R, Sapkal V, Zamre G (2009) Int J Chem Sci 7:681–688
42. Kalita RD, Nath Y, Ochubiojo ME, Buragohain AK (2013) Coll Surf B 108:85–89
43. Zhao T, Chen Z, Lin X, Ren Z, Li B, Zhang Y (2018) Carbohydr Polym 184:164–170

44. Merci A, Urbano A, Grossmann MVE, Tischer CA, Mali S (2015) Food Res Int 73:38–43
45. Xiu H, Ma F, Li J, Zhao X, Liu L, Feng P, Yang X, Zhang X, Kozliak E, Ji Y (2020) Powder Technol 364:241–250
46. Krishnan VN, Ramesh A (2013) IOSR J Appl Chem 6:18–23
47. Garba ZN, Lawan I, Zhou W, Zhang M, Wang L, Yuan Z (2019) Sci Total Environ 690:867–877
48. Sonia A, Dasan KP (2013) Carbohydr Polym 92:668–674
49. Neto WPF, Silvério HA, Dantas NO, Pasquini D (2013) Ind Crop Prod 42:480–488
50. Tarchoun AF, Trache D, Klapötke TM (2019) Int J Biol Macromol 138:837–845
51. Luddee M, Pivsa-Art S, Sirisansaneeyakul S, Pechyen C (2014) Energy Proc 56:211–218
52. Sheng S, Meiling Z, Chen L, Wensheng H, Zhifeng Y (2018) Waste Manag 82:139–146